Fe-Ni deposition may be included in the film and increase the resistivity. One can also notice that a field of 2 kOe does not correspond to the saturation field of our multilayers. Hence a larger MR ratio can be expected at higher fields.

Acknowledgments

It is a pleasure to thank Dr. J-P. Chevalier for critically reading the manuscript.

Manuscript submitted Dec. 1, 1995; revised manuscript received Feb. 23, 1996.

Centre d'Etudes de Chimie Metallurgique, CNRS, assisted in meeting the publication costs of this article.

REFERENCES

1. M. N. Baibich, J. M. Broto, A. Fert, F. Nguyen Van Dau, F. Petroff, P. Eitenne, G. Creuset, A. Friederich, and J. Chazelas, *Phys. Rev. Lett.*, **61,** 2472 (1988).
2. S. S. P. Parkin, R. Bhadra and K. P. Roche, *ibid.*, **66,** 2152 (1991).
3. S. S. P. Parkin, Z. G. Li, and D. J. Smith, *Appl. Phys. Lett.*, **58,** 2710 (1991).
4. M. Dariel, L. H. Bennet, D. S. Lashmore, P. Lubitz, W. L. Lechter, and M. Z. Harford, *J. Appl. Phys.*, **61,** 4067 (1987).
5. M. Alper, P. S. Aplin, K. Attenborough, D. J. Dingley, R. Hart, S. J. Lane, D.S. Lashmore, and W. Schwarzacher, *J. Magn. Magn. Mater.*, **126,** 8 (1993).
6. M. Alper, K. Attenborough, V. Baryshev, R. Hart, D. S. Lashmore, and W. Schwarzacher, *J. Appl. Phys.*, **75,** 6543 (1994).
7. K. D. Bird and M. Schlesinger, *This Journal,* **142,** L65 (1995).
8. J. Yahalom and R. Intrater, *J. Mater. Sci. Lett.*, **12,** 1549 (1993)
9. L. T. Romankiw and J. D. Olsen, in *Proceedings of the Symposium on Magnetic Materials, Processes and Devices,* L. T. Romankiw and D. A. Herman, Jr., Editors, PV 90-8, p. 339, The Electrochemical Society Proceedings Series, Pennington, NJ (1990)
10. K. Attenborough, R. Hart, S. J. Lane, M. Alper, and W. Schwarzacher, *J. Magn. Magn. Mat.*, **148,** 335 (1995)
11. L. J. Van der Pauw, *Philips Res. Rep.*, **13,** 1 (1958).
12. A. Brenner, in *Electrodeposition of Alloys,* Vol I, p. 149, Academic Press, Inc., New York (1968).
13. J. Horkans, *This Journal,* **128,** 45 (1981).
14. S. N. Srimathi and S. M. Mayanna, *J. Appl. Electrochem.*, **16,** 69 (1986).
15. P. C. Andricacos, C. Arana, J. Tabib, J. Dukovic, and L. T. Romankiw, *This Journal,* **136,** 1336 (1989).
16. J. Hessami and C. W. Tobias, *ibid.*, **136,** 3611 (1989).
17. T. Akiyama and H. Fukushima, *I.S.I.J. Intl,* **32,**787 (1992).
18. D. L. Grimmet, M. Schwartz, and K. Nobe, *This Journal,* **140,** L65 (1993).
19. M. Matlosz, *ibid.*, **140,** 2272 (1993).
20. K. Y. Sasaki and J. B. Talbot, *ibid.*, **142,** 775 (1995).
21. N. Lebbad, E. Chaînet, J. Voiron, and B. Nguyen, in *Proceedings of 44th I.S.E Meeting,* p. 352, Berlin, 1993.
22. W. B. Pearson, in *Handbook of Lattice Spacings and Structures of Metals,* Pergamon Press, New York (1967).
23. S. S. P. Parkin, *Appl. Phys. Lett.*, **60,** 512 (1992).
24. K. Noguchi, S. Araki, T. Chou, D. Miyauchi, Y. Honda, A. Kamijima, O. Shinoura, and Y. Narumiya, *J. Appl. Phys.*, **75,** 6379 (1994).
25. Th. G. S. M. Rijks, R. Coehoorn, J. T. F. Daemen, and W. J. M. de Jonge, *ibid.*, **76,** 1092 (1994).

Isolated Submicrometer Filaments Formed by Silicon Anodization in HF Solutions

O. Teschke* and D. M. Soares

Instituto de Fisica, UNICAMP, 13081-970, Campinas, SP, Brazil

ABSTRACT

Porous silicon nanocolumn formation is the result of the merging of nearest-neighbor nanopores. In this paper we describe isolated submicrometer filaments formed by silicon anodization in HF solutions. The merging of nearest-neighbor pores may result in the formation of isolated submicrometer silicon filaments. The filament formation is explained by a model which takes into account filament wall layer passivation by hydrogen atoms. The formation of one isolated wire structure is a consequence of the pore diameter enlargement resulting from the available area decrease with etching time.

Despite its discovery as late as 1956 by Uhlir,[1] the morphology and structures achievable with silicon anodization have received detailed consideration only over the last decade.[2-7] The electrochemical dissolution of silicon wafers at low current densities in HF-based solutions can be used to generate an array of extremely small holes. The shape and size of silicon nanostructures left after partial electrochemical dissolution has been recently published.[8-11]

Microstructures in silicon are increasingly being used for the fabrication of mechanical and electrical devices. The purposes of this letter is to draw attention to the self-limiting etching process that produces silicon submicrometer filament structures. The idea is to use etching at high current density which results in wide etched holes. The overlapping of these holes will result in isolated silicon filaments.

Samples were prepared by etching silicon wafers in an electrochemical cell previously described.[11] The substrates were n-type, 0.009 Ω cm, <100> oriented silicon slabs. Retangular pieces, 2 × 0.5 cm, were cut from a 2 in. diam wafer before anodization. After 20 min anodization at a 100 mA current (initial area 1.0 cm^2), a substantial decrease of the slab dimensions is observed (final area ~0.5 cm^2) resulting in curved contour substrates and an increase in the current density. The constant current was generated by an EG&G Princeton Applied Research 273A galvanostat/potentiostat. The sample edges were gently touched by a 400 mesh transmission electron microscopy (TEM) specimen (palladium-coated) grid. Fragments of the silicon slab tip were transferred to the specimen grid by capillary adhesion. The grid was then dried and inserted into the TEM for study within 24 h of the anodic fabrication of the slab. TEM examinations were carried out in a Zeiss CEM902 microscope using 80 keV electrons and equipped with an image intensifying camera.

Figure 1 shows an electron energy loss spectrum image of a wedge-etched silicon wafer. The image was formed by the absorption spectra at 42 eV. Observe that the structure of the pores forms an array of parallel pipes approximately 3 μm long. This micrograph suggests that silicon of low porosity can be adequately approximated by an array of noninteracting cylindrical pores of fixed diameters since the structure is formed by an array of independent holes. Percolation corresponding to a porosity $p_c = \pi/4 = 0.785$ is schematically represented in Fig. 2. For cylindrical pores, porosities much greater than p_c promote substantial merging of the nearest-neighbor pores and consequently the physical isolation of silicon columns. The profile of the resulting structure is shown by the shaded area in Fig. 2.

An isolated etched wire is shown in Fig. 3a. This submicrometer filament is formed by the central region which is thicker than its edges and is not transparent to the electron beam, consequently shown as a dark region. The observed wire cross section shown in Fig. 3a, is in agreement with the schematic diagram of an isolated silicon column shown in Fig. 2. The observed filament shape is

* Electrochemical Society Active Member.

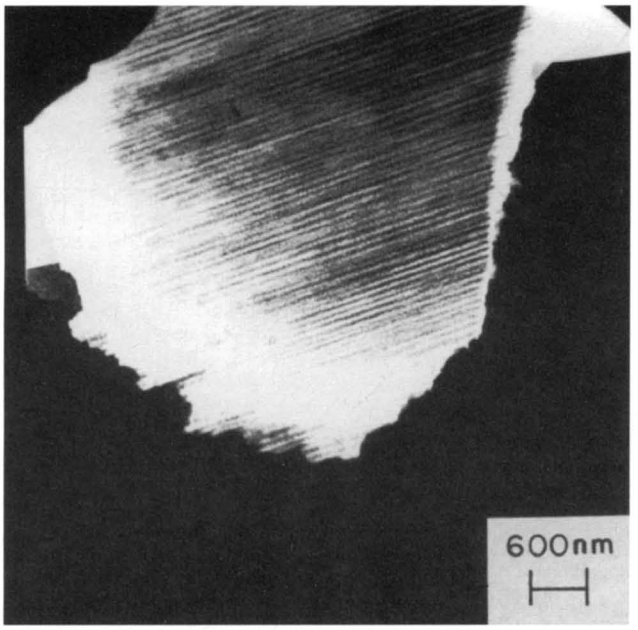

Fig. 1. Electron energy loss spectroscopy image recorded on a transmission electron microscope for an absorption spectra of 42 eV. Pores form an array of parallel ~3 μm long pipes. The pattern was formed by silicon anodization of <100> n-type silicon with current density ~180 mA/cm^2 in 50% HF alcoholic solution.

then consistent with the one proposed by the percolation model. Other submicrometer filaments are shown in Fig. 3b and c.

We believe that the formation of the array of pores shown in Fig. 1 is a consequence of the passivation of the silicon surface during silicon anodization by hydrogen.[12,13] In order to understand pore formation, it is necessary to deal with the mechanism of the anodic surface dissolution. At the onset of the anodic current, the silicon surface is all H covered.[14] The field built up across the space-charge layer moves holes toward the surface at kinks, defects, or tensioned regions. This induces a nucleophilic attack on the Si-H bonds by F^- (or HF_2^-) ions, forming SiF_2 groups at these sites and ions (H^+) in the solution. The Si-Si back bonds of the SiF_2 groups are stretched due to the fluorine electronegativity allowing the insertion of F^- (or HF_2^-) ions. The reaction transfers the SiF_2 groups from the surface to the solutions, and forms two new Si-F bonds which react again as

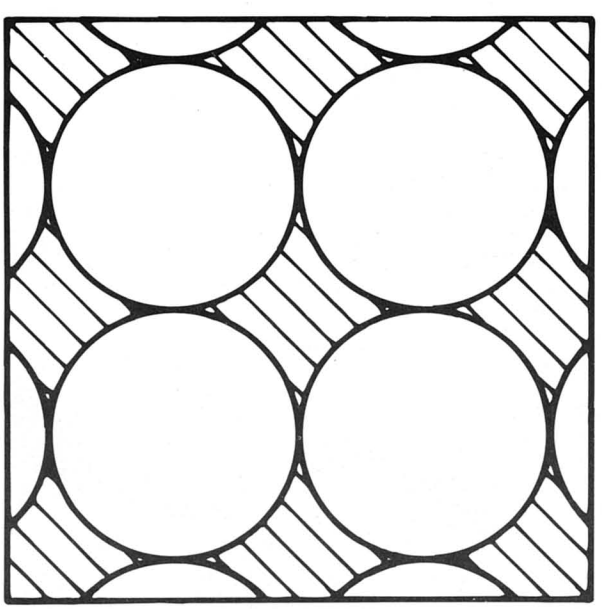

Fig. 2. Array of cylindrical holes showing a merging of nearest neighbor pores. Isolated silicon columns have a cross section shown by the dashed area.

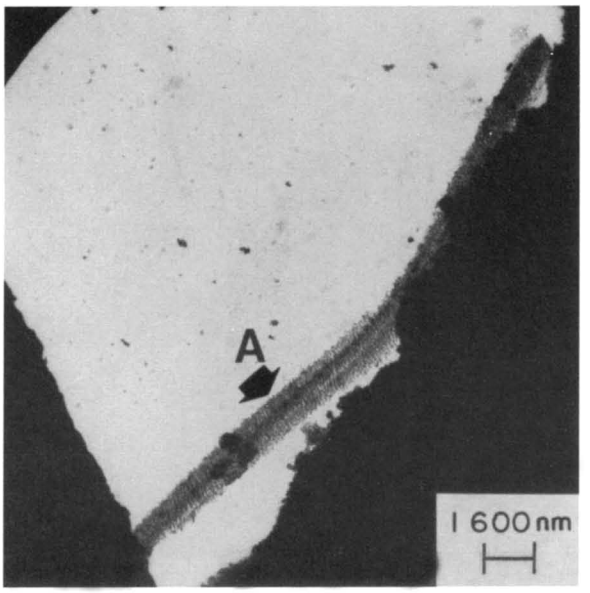

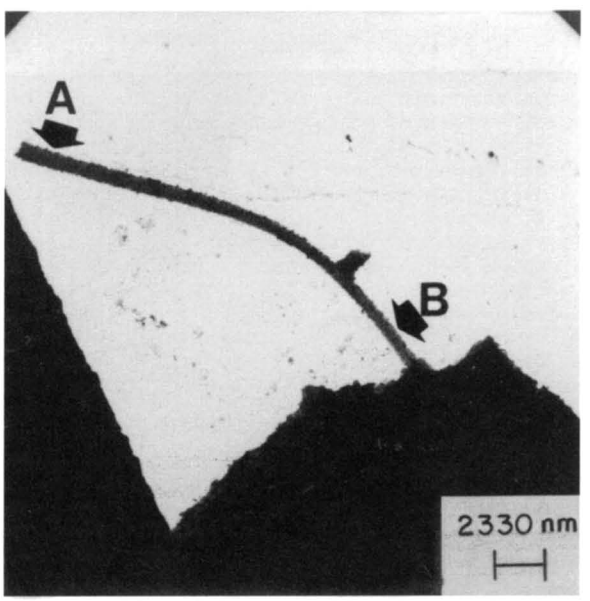

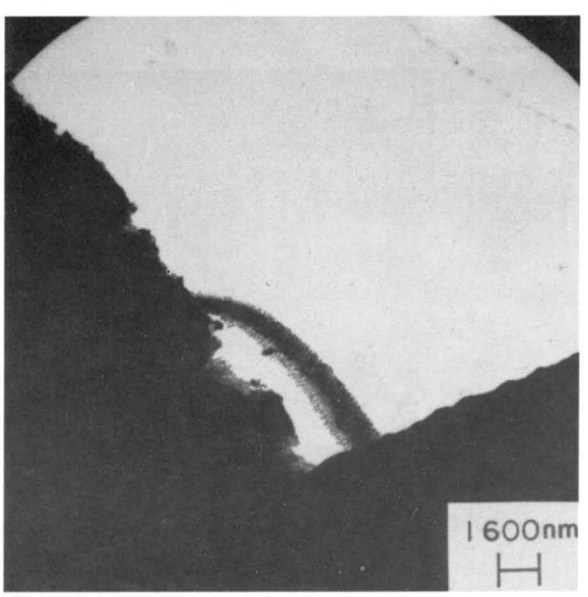

Fig. 3. Isolated etched silicon submicrometer filaments. (a, top) The filament cross section indicated by A is similar to the dashed area in Fig. 2. (b, center) B indicates a region closer to the substrate then A. (c, bottom) Curved micrometer filament.

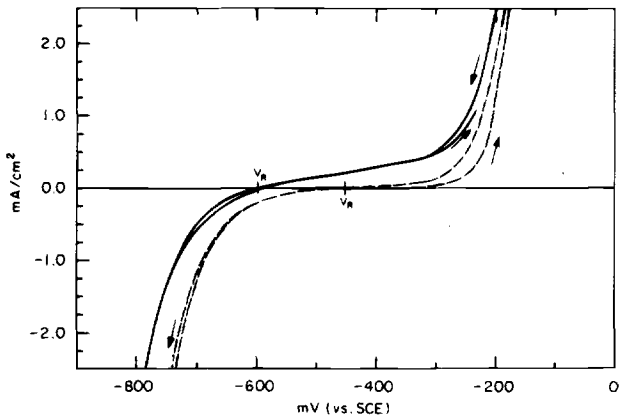

Fig. 4. Current *vs.* electrode potential curves for illuminated, 0.009 Ω cm, n-type <100> oriented silicon samples. The full-line curves correspond to a silicon surface and the dashed line curves were obtained after the porous structure formation. After the first cathodic scan the zero current potential (V_R) shifts gradually to more cathodic values. V_R is −420 mV for silicon and −625 mV for the etched structure.

$$[Si_N]SiF_2 + 2h^+ + 2F^2_{Sol.} \rightarrow [Si_{N-1}]SiF_2 + (SiF_2)_{Sol.} \quad [1]$$

The above reaction changes the surface geometry and the electric field distribution so that the next hole transference will preferentially occur at this location thus enlarging the "pore." The intermediary product $(SiF_2)_{Sol.}$ reacts rapidly with HF, forming H_2 and SiF_4.[7]

Figure 4 shows the current *vs.* voltage curves of an n-type, 0.009 Ω cm <100> silicon sample (full line), and after porous layer formation (dashed line). The process of pore formation shifts the zero current potential (V_R) to more positive potentials, increases the anodic reverse current, I_R, and decreases the hydrogen evolution reaction (HER) rate (smaller slope of the *I vs. V* curve at potentials more negative than V_R) as shown in Fig. 4 (dashed line). The electrochemical potential, V_R, corresponds to the H_2 oxidation reaction, which occurs at the Si-H surface bonds covering the electrode surface, as follows[13]

$$(Si\text{-}H)_{Crys.} + (H_2)_{Sol.} \leftrightarrow (Si\text{-}H)_{Crys.} + 2e^-_{Crys.} + 2H^+ \quad [2]$$

This allows the H_2 oxidation reaction to inject electrons into surface states and H^+ into the solution resulting in an anodic current of ≈0.4 mA/cm² at $V = -400$ mV, Fig. 4. The apolar characteristic of the Si-H bond enhances the chemical stability of the Si surface against attacks by polar molecules like H_2O, HF, etc. It also decreases the inverse HER rate.

At potentials more positive than V_R, a second electrochemical wave is observed, which corresponds to the silicon dissolution reaction (SDR), where H_2 is the reaction subproduct.

A spatially variable corrosion rate distribution, where the H-covered sites are passivated by the $H_2 \rightarrow 2H^+ + 2e^-$ reaction, which locally lowers the electrode potential, is responsible for the structure formation. An increase in the current density results in an increase in the F-covered sites which correspond to the conducting sites. Highly conductive silicon substrates facilitate the electron transfer from H-covered sites to the F-covered sites, enhancing the SiF_2 formation.

Porous silicon is formed by an interconnected[2,9,10] skeleton structure of silicon nanowires. The structure reported in this paper is formed by isolated submicrometer filaments. Both structures are generated by the anodization of silicon in HF solutions, the difference being the etching current density; high current densities favor the formation of wide pores. However, the description must also explain why isolated structures are observed instead of an array of filaments as would be expected when considering pore merging in the structure observed in Fig. 1. For a rectangular slab 1 cm long and 0.5 cm wide, anodized at a current density of 100 mA/cm², there is a substantial decrease of the slab area after 20 min of anodization. Consequently, as the etching duration increases, the effective contact area with the electrolyte decreases resulting in a decrease in the filament diameter with time. The wires are thinner in regions closer to the substrate than at the top of the surface, as shown in Fig. 3b, where the initial filament diameter is indicated by A and the final diameter by B. This observed filament thinning effect is the result of an imposed total constant current and is responsible for the formation of single isolated wires since only a few structures will remain attached to the substrate after a given anodization period. Most of the wires have such a small diameter close to the substrate that they will break loose.

In conclusion, submicrometer filament formation in n-type silicon immersed in hydrofluoric acid under anodic bias is demonstrated and the resulting structures are characterized. The wire formation is explained by a model which takes into account hydrogen atoms which form a passivating sidewall layer.

Acknowledgments

The author would like to thank L. O. Bonugli and J. R. Castro for technical assistance and R. M. Sassaki for assistance with electron microscopy techniques. This work was supported by CNPq 520060/93-8, FAPESP 93/0961-5 and 93/2412-9.

Manuscript submitted Feb. 1, 1996; revised manuscript received Feb. 23, 1996.

FUNCAMP assisted in meeting the publication costs of this article.

REFERENCES

1. A. Uhlir, *Bell Sys. Tech. J.*, **35,** 333 (1956).
2. L. T. Canham, *Appl. Phys. Lett.*, **57,** 1046 (1990).
3. M. I. J. Beale, J. D. Benjamin, M. J. Uren, N. G. Chew, and A. G. Cullis, *J. Cryst. Growth*, **73,** 622 (1985).
4. L. G. Earwaker, J. P. G. Farr, P. E. Grzeszezyk, I. Sturland, and J. M. Keen, *Nucl. Instrum. Methods Phys. Rev.*, **B9,** 317 (1985).
5. G. Bomchil, A. Halimaoui, and R. Herino, *Microelectron. Eng.*, **8,** 293 (1988).
6. R. L. Smith, S. F. Chuang, and S. D. Collins, *J. Electron. Mater.*, **17,** 533 (1988).
7. R. Memming and G. Schwandt, *Surf. Sci.*, **4,** 109 (1966).
8. A. G. Cullis and L. T. Canham, *Nature*, **353,** 335 (1991).
9. O. Teschke, F. Alvarez, L. R. Tessler, and M. U. Kleinke, *Appl. Phys. Lett.*, **63,** 1927 (1993).
10. O. Teschke, F. Galembeck, M. C. Gonçalves, and C. U. Davanzo, *ibid.*, **64,** 3590 (1994).
11. O. Teschke, M. C. Gonçalves, and F. Galembeck, *ibid.*, **63,** 1348 (1993).
12. D. M. Soares, M. C. dos Santos, and O. Teschke, *Chem. Phys. Lett.*, **242,** 202 (1995).
13. O. Teschke, M. C. dos Santos, M. U. Kleinke, D. M. Soares, and P. S. Galvão, *J. Appl. Phys.*, **78,** 590 (1995).
14. G. W. Trucks, K. Raghavachari, G. S. Higashi, and Y. J. Chabal, *Phys. Rev. Lett.*, **65,** 504 (1990).